

# Chinese lockdown as aerosol reduction experiment

Hans VON STORCH<sup>a,b,\*</sup>, Beate GEYER<sup>a</sup>, LI Yan<sup>c</sup>, Volker MATTHIAS<sup>d</sup>, Burkhardt ROCKEL<sup>a</sup>

<sup>a</sup> Institute of Coastal Systems, Helmholtz-Zentrum Geesthacht, Geesthacht, 21502, Germany

<sup>b</sup> Ocean University of China, Qingdao, 266100, China

<sup>c</sup> College of Life Sciences and Oceanography, Shenzhen University, Shenzhen, 518061, China

<sup>d</sup> Institute of Biogeochemistry in Coastal Seas, Helmholtz-Zentrum Geesthacht, Geesthacht, 21502, Germany

Received 12 October 2020; revised 18 January 2021; accepted 5 March 2021

Available online 13 March 2021

## Abstract

The lockdown of large parts of Chinese economy beginning in late January 2020 lead to significant regional changes of aerosol loads, which suggests a reduction of backscatter and consequently a regional warming in the following months. Using local data and a numerical experiment with a limited area model, we have examined how strong this response may have been. The observed (local and reanalysis) observations point to a warming of less than 1.0 K, the simulations to a warming of the order of 0.5 K. These numbers are uncertain, because of large-scale natural variability and an ad-hoc choice of aerosol optical depth anomaly in the simulation. Thus, the result was, in short, that there was actually a weak warming of a few tenth of degrees, while noteworthy changes in circulation or in precipitation were not detected. More specifically, we found that at selected central China stations temperatures were found to be higher than in previous two years. This warming goes with a marked diurnal signal, with a maximum warming in the early afternoon (06 UTC), weakest at night (18 UTC). This may be related to a general warming of large swaths of Asia (including Siberia, which is not related to local aerosol forcing). Indeed, also the stations outside the immediate strong lockdown region are showing warming, albeit a weaker one. Thus, the difference 2020 minus 2019/2018 may overestimate the effect. The ad-hoc series of numerical experiments indicates that the simulated changes are robust and suffer little from internal dynamical variability. In particular, the overall reduction of the aerosol optical depth does not lead to phases of larger intermittent divergence among the model simulations, irrespective of the aerosol load. Instead, the simulations with reduced anthropogenic aerosol load show more a mere locally increased temperature. This may indicate that the aerosol effect is mostly thermodynamic in all local air columns in the region.

**Keywords:** Lockdown; China; Aerosol; Climate

## 1. Introduction

On April 22, 2020, the news agency Bloomberg<sup>1</sup> wrote: “Restrictions on travel and non-essential business over the past weeks to control the spread of Covid-19 have meant

dramatically cleaner air for some of the world's most polluted cities. ... Wuhan, the Chinese city in the epicenter of the Covid-19 outbreak, was put in a 10-week lockdown, keeping 11 million residents in their homes and shutting down manufacturing facilities. During the ... peak lockdown period, Wuhan's PM2.5 level went down 44% from 2019.

Physical understanding (McCartney, 1976) as well as observational evidence (e.g., Hong et al., 2020; Jung et al., 2019) suggest a local or regional link, with additional aerosols causing a cooling because of the reflective properties of the aerosols. Thus, we expect a gradual warming in the neighborhood of the industrial centers, where the lockdown was instituted.

\* Corresponding author. Institute of Coastal Systems, Helmholtz-Zentrum Geesthacht, Geesthacht, 21502, Germany.

E-mail address: [hvonstorch@web.de](mailto:hvonstorch@web.de) (VON STORCH H.).

Peer review under responsibility of National Climate Center (China Meteorological Administration).

<sup>1</sup> <https://www.bloomberg.com/graphics/2020-pollution-during-covid-19-lockdown/> (9 August 2020).

With Wuhan beginning on January 23, 2020, other Chinese cities including Beijing followed to it, so that a widespread reduction of the Chinese emission of anthropogenic substances took place.

This reduction lead to changes compared to the previous year in PM<sub>2.5</sub> of −24.9%, with maxima in the Yangtze River Delta. NO<sub>2</sub> was reduced by 25%–30% in the Beijing-Tianjin-Hebei region, Pearl River Delta and the Yangtze River Delta (Yue et al., 2020) based on the analysis of surface monitoring sites and satellite retrievals. For further details on the effect on air quality, refer to He et al. (2000).

Lee et al. (2021) calculated the difference of Aerosol Optical Depth at 550 nm for February 2020 minus February composite over years 2016–2019 using Suomi National Polar-orbiting Partnership (SNPP) Visible and Infrared Imaging Radiometer Suite (VIIRS) NASA standard Level-3 monthly deep blue aerosol data – and found in East Asia a reduction of up to 30%.

Another source of information about the presence of man-made aerosols is provided by the total aerosol optical depth (AOD) in the MERRA2 reanalysis (Gelaro et al., 2017). This AOD considers all aerosols, both natural and anthropogenic. The reanalysis incorporates local AERONET-data (Holben et al., 1998) as well as various satellite products, albeit only if cloud cover permits. For March, for four Asian large urban conglomerates, among them Beijing and Wuhan, the developments of AOD since 1980 show instationary behavior, with maxima in Wuhan and Beijing in about 2010, and a decay since then; a marked decay of the 2020 levels compared to the 2019 levels is not visible. While this may point to some deficiencies of the reanalysis, related to the inclusion of actual emission estimates in the Goddard Chemistry, Aerosol, Radiation, and Transport model (GOCART) model (Chin et al., 2002), it sheds light on the difficulty to determine the change of anthropogenic aerosol load.

We conclude that there was a massive reduction of the anthropogenic aerosol optical depth in the industrial regions of China, which is difficult to quantify. It is in any case significant, of the order up to 50% or so.

The lockdown in China provides an excellent opportunity to study the effect of changing aerosol loads on the regional climate; a kind of unintended experiment, so to speak. The good ‘experimental’ thing is that it is a relatively isolated but large area, with a relatively strong signal. In other parts of the world, such as Northern Italy (Rugani and Caro, 2020), also experiments were done, but in a smaller region, where policies for air pollution have been implemented for a longer time.

The interest in the effect of a significant reduction of anthropogenic aerosol load was sparked by the observation that in the Baltic Sea region the warming in the past decades was higher than what was suggested by climate change simulations subject to only changing GHG levels (Barkhordarian et al., 2016). The effect in the Baltic Sea region was moderate in winter, but strong in summer. It has been speculated that this difference could be due to the disregard of the simultaneous

massive decrease in anthropogenic aerosol load. The case studied here, in winter in central China was hoped to shed light on this discrepancy, but the evidence seem hardly conclusive; in this case, the reduction of the aerosol load is increasing temperatures by a few tenth of a degree, while in case of the Baltic Sea, the ‘unexplained’ warming in the observations, possibly related to also anthropogenic aerosol reduction, is smaller in winter – with the Baltic Sea region winter enjoying less short wave radiation than in China, due to the latitudinal shift of 10°–20° latitude.

While there have been many studies on the effect of the lockdown on the air quality, few are available at this time about the regional climatic effect. This is likely related to the short time since the event so that data collection and, possibly modelling efforts, need some time to manifest themselves in publications. One case is Weber et al. (2020), with results consistent with those reported in this article.

There rarely have been specific studies in the literature, to our knowledge, dealing with the recent lockdown effect in China on the regional climate. We try to fill this gap.

Using the opportunity, we try to determine the effect of a sudden and regionally widespread reduction of anthropogenic aerosols. Our tools, data and model, are introduced in Section 2. In the Results Section 3, we first examine the variations of temperature at a series of monitoring sites through China from January to April 2020, and then examine the output of a numerical experiment with a regional atmospheric model, when subject to a prescribed reduction of anthropogenic aerosols.

## 2. Data and models

### 2.1. Data

From the archive of China Meteorological Administration (<http://data.cma.cn>) we got 4-daily temperature readings from a series of stations (Fig. 1) for January–April 2020. We also used the JRA55 reanalysis (Kobayashi et al., 2015) of January 1990–April 2020.

### 2.2. Dynamical model set-up

For our experiments we used the limited area model COSMO-CLM (Consortium for Small-scale Modelling model in Climate Mode; Rockel et al., 2008) based on the regional weather prediction model COSMO, formerly called LM (Local Model; Steppeler et al., 2003). The model has been applied and its performance has been shown over China and East Asia in a couple of publications (Wang et al., 2013; Bucchignani et al., 2014, 2017; Zhou et al., 2016; Li et al., 2018; Yu et al., 2020) and also specifically with focus on Bohai and Yellow Sea (Li, 2017; Li et al., 2016a, 2016b, 2020). Li et al. (2018) evaluated the model CCLM over China and assessed the added value of CCLM to the driving GCMs. The performance of the CCLM was in general satisfactory, however, with a strong seasonal variability (e.g. temperature

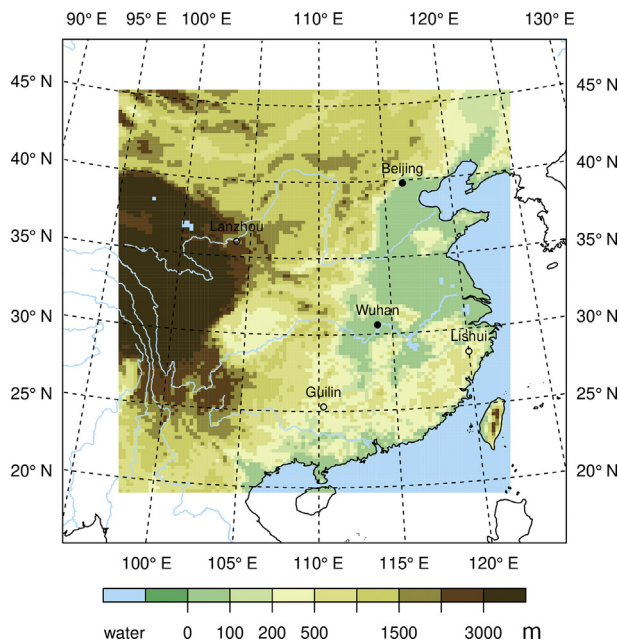


Fig. 1. Geographical map of the model domain of COSMO-CLM. (In the colored inner part of the map the simulation is unconstrained, while in the white 'sponge zone' the model is partly constrained by a nudging towards the driving reanalysis. The map does not imply any assertions on political boundaries or jurisdictions).

showed better results in summer than in winter). Regarding the added value, the CCLM outperforms the GCMs in winter for most regions but less clearly in summer.

For estimating the effect of the reduced presence of anthropogenic aerosols in a dynamical model experiment, it would be best if we had the time- and space dependent aerosol optical depth. As outlined before, we do not have a reliable and complete estimate of this. Therefore, we have done an idealized experiment with an ad-hoc chosen forcing.

Specifically, we have performed a series of three pairs of numerical simulations with the COSMO-CLM. Each pair consists of a 'control run' (ctrl X), with a monthly mean aerosol distribution, representing the influence of aerosols on the radiative transfer, and an 'experimental' run (aer X), which is identical to the control run except for a 50% reduction of the anthropogenic AOD throughout the model area. Here, following the recommendations from Schultze and Rockel (2018) the aerosol distribution MAC-v2 (an update of the MAC-v1 climatology, Kinne et al., 2013) is implemented in the regional model. This aerosol climatology includes the monthly means of aerosol optical properties (aerosol optical depth, single scattering albedo and asymmetry factor) on a  $1^\circ \times 1^\circ$  grid at a monthly resolution. For the year 2019 the aerosol distribution is used in the model as is. For January to April 2020 the data are not yet available and therefore the AOD values from 2019 were taken as a first guess.

The model region is shown in Fig. 1, covering most parts of China. At lateral boundaries reanalysis states, as given by the JRA55 reanalyses (Kobayashi et al., 2015), are prescribed. In the diagram the traditional sponge-zone is marked in white.

Spectral nudging is not provided; only lateral boundary conditions are considered after the relaxation proposed by Davies (1976).

The model is discretized on a horizontal rotated grid with mesh length of about  $0.22^\circ$  (approximately 22 km), and by 40 vertical levels in terrain-following hybrid height coordinates. The effect of aerosols on radiation is included in the delta-two-stream radiation scheme by Ritter and Geleyn (1992) implemented in the COSMO-CLM. The radiation scheme uses the aerosol optical depth, single scattering albedo and asymmetry factor given by the MAC-v2 climatology. The stipulated aerosol distributions in the four months, January to April, as given by MacV2ctl exhibit a regional maximum, centered in central China, covering  $105^\circ$ – $120^\circ$  E and  $25^\circ$ – $40^\circ$  N. Maximum levels are determined for March. The reduction of anthropogenic aerosols by 50% results in concentration maps similar to the full maps (Fig. A1). No indirect effect of aerosols is considered, since the cloud parameterization in COSMO-CLM does not take into account changes in aerosols, yet.

The three pairs of simulations differ with respect to the time of initialization, namely 1 December, 1 November and 1 July 2019. The interval variability from January to April 2020 is evaluated by analyzing the differences  $\Delta X = \text{ctrl } X - \text{aer } X$ ,  $X = 1, 2, 3$ .

### 3. Results

#### 3.1. Analysis of in-situ and reanalysis data

In this section we study how different the regional January to April 2020 climate was compared to previous years.

- In late January the lockdown began in Wuhan; thus, the effect of the lockdown is expected to be minor in this month. The China-mean temperature was  $1.4^\circ\text{C}$  warmer than 'in normal years' (Jiang et al., 2020).
- In February 2020 the lockdown was in full swing – in this month the monthly mean temperature in China was higher by  $1.6^\circ\text{C}$  (Cao et al., 2020).
- In March, temperatures were  $2^\circ\text{C}$  warmer (Zhou and Zhang, 2020).
- April 2020 showed no general warming, but temperatures close to normal (Guan et al., 2020). In the early part of the month, many stations saw a 'sharp drop in temperature'.

Figure 2 shows the temperature development, as daily average, for Wuhan in 2020 and the two previous years. Because of the instationarity of the aerosol-load mentioned in the Introduction, we decided to do here a comparison with only two earlier years, when we may expect to see differences related to the anthropogenic aerosol load and the unavoidable natural variability.

In January, the 2020 temperature does not look substantially different for the previous two years, but both February and March were 2020 warmer than in the previous years. April is begun with a strong cooling, and later values similar to the

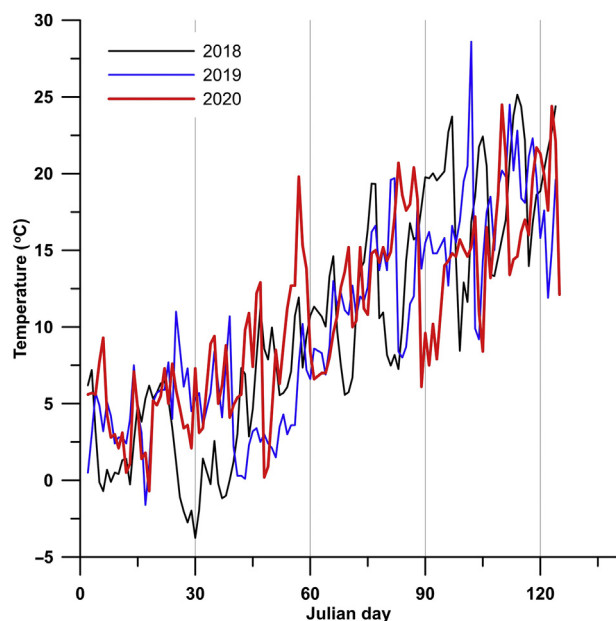


Fig. 2. Daily average of surface air temperature at Wuhan in 2018, 2019 and 2020 during January to April. Julian days count the number of days beginning on 1 January.

previous years. Fig. 2 substantiates the general assessment given above, including the decrease of the warming in April.

In principle any warming may be due to the synoptic ‘weather’ variability or to local changes reflecting the reduction of aerosol presence. The former would be of larger-scale, and mostly in the northern part of the region, and changing from month to month. The latter is expected to reflect the scale of the aerosol reductions, centered over the regions with maximum industrial activity, where the lockdown led to the largest local forcing anomalies. Since the lockdown region was mostly the same during spring 2020, the warming is also expected to be strongest in that region. We find, in Fig. 3, the relatively small industrial region to be warmer than the more remote

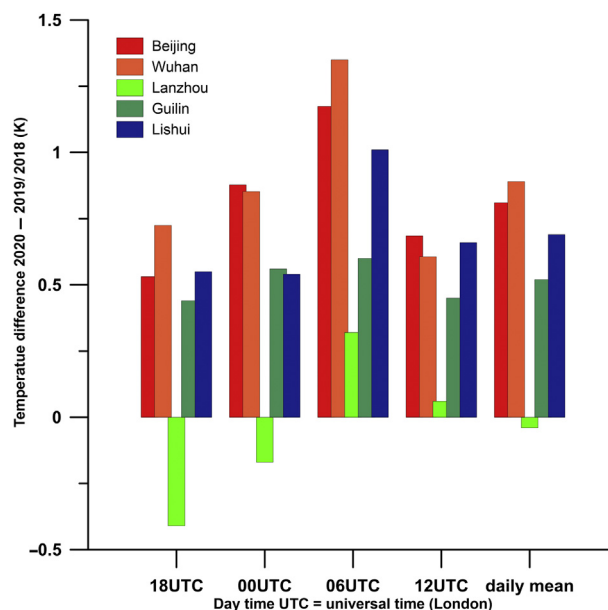


Fig. 4. Mean differences of locally reported air temperatures (2020 minus 2019/2018) at five locations at different times of day and as daily mean, both from 6-hourly data for January to April.

surrounding, in all three months. Also, an inspection of temperature anomalies at Wuhan and Beijing (serving as examples), show that the warming (difference to long term mean) at these locations in 2020 was increased compared to the previous years (not shown). Further north, where the synoptic activity with travelling tropospheric waves is stronger, a variable pattern of warming is found, consistent with the hypothesis of synoptic variability and advective short term warming.

Thus, we conclude that the observational evidence, even if contaminated by the effect of synoptic variability mostly in the Northern part of China, supports the basic hypothesis, namely that the lockdown would lead to a regional warming, or more precisely, to a reduction of aerosol related cooling.

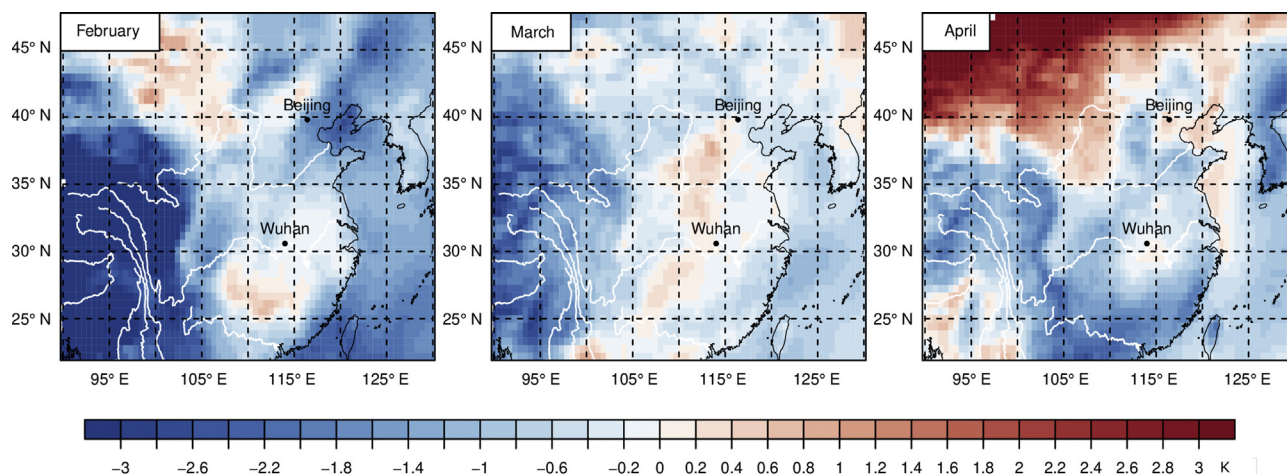


Fig. 3. Maps of the differences of monthly mean temperature anomalies, 2020 minus 1990–2019, throughout the region minus the anomaly in Wuhan. Red colored regions experienced in 2020 positive temperature deviations from the ‘normal’ larger than the warming in Wuhan. In the same way, bluish regions have been relatively colder in 2020 than in previous years compared to what has been recorded in Wuhan (Derived from JRA55 reanalysis data).



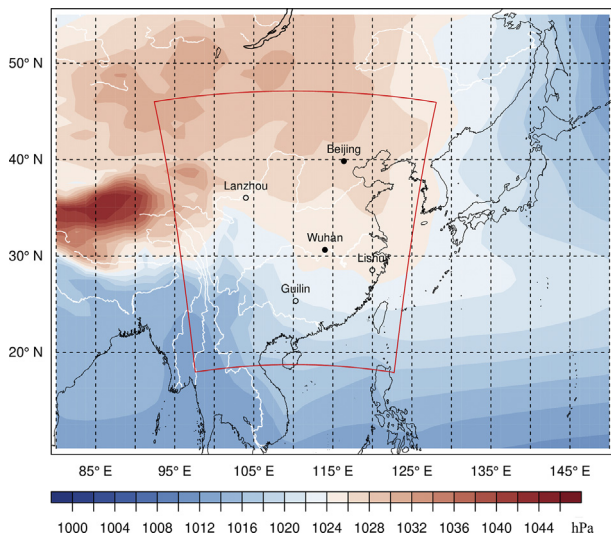


Fig. 5. Mean surface air pressure (reduced to mean sea level) distribution in February 2020 as given by JRA55 reanalysis (The red line marks the model domain of the aerosol experiments).

This is substantiated by Fig. 4, which shows the temperature means for the months January, February, March and April in 2020, 2019 and 2018 – for the 4 daily recording times, namely 6 UTC, 12 UTC, 18 UTC and 00 UTC (corresponding to local times of 13:00, 19:00, 01:00 and 07:00 CST). The station Lanzhou is in the far West, outside of reach of the lockdown effect, Lishui is a station near the coast southwest of Shanghai, and Guilin is a southern station far off the coast (Fig. 1).

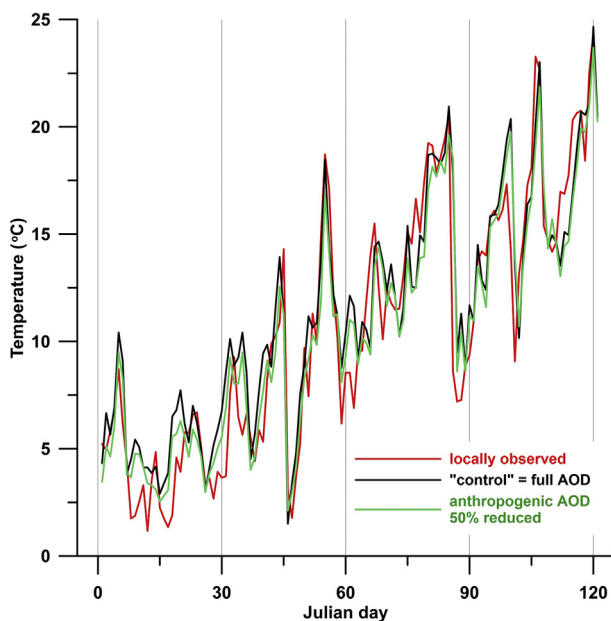


Fig. 6. Temporal development of surface air temperature in Wuhan during January to April 2020. The local observational data (black) were discussed in the previous section; the red and blue lines describe the developments in the first pair of simulation, aer1 and ctl1. Note that the lockdown began in Wuhan on 23 January, while the reduction of the aerosol load in the model began on January 1 (Julian days count the number of days commencing on 1 January).

All stations, except for Lanzhou, show a warming in all months, with maximum values at Beijing time of 13:00 CST (06 UTC) at the two locations strongly affected by the lockdown, namely Wuhan and Beijing, whereas the less affected stations Guilin and Lishui go with a smaller warming. During night, as is to be expected, the warming effect is weakest. This diurnal pattern is evidence that really the reduction of aerosol is at work.

The warming is largest at the centers of the lockdown, with a maximum up to 1.3 K at noontime, and a minimum of about 0.6 K at night. In the wider neighborhood, such as Guilin and Lishui, the warming ranges from less than 0.5 K at night to 1 K when solar radiation is strongest. Because of the unknown contribution by synoptic advection, these numbers are likely upper limits, but claiming an aerosol-reduction related warming between 0.5 K and 1 K is justified.

### 3.2. Numerical experimentation with regional dynamical model

In previous similar simulations (such as Weisse et al., 2000, or Geyer et al., 2020) the different members of the ensemble were characterized by long episodes of very similar developments, interrupted by episodes of several days with strong differences, which were reflected in different dynamical developments, thus different circulations and precipitation. In these cases, the model area was located at the end of the North Atlantic storm track with the emergence of unstable dynamical states. In this case, with the model area covering mainland China, mostly stable winter-monsoon conditions prevail, as demonstrated by the surface air pressure distribution in February 2020 (Fig. 5). Thus, not unexpectedly (Geyer et al., 2020), noteworthy deviations in the circulation did not emerge (no intermittent divergence in phase space, not shown), and the intra-ensemble variability is small and mostly visible in local temperatures. Thus, in the following we discuss only the impact of changed aerosol-presence on surface temperature.

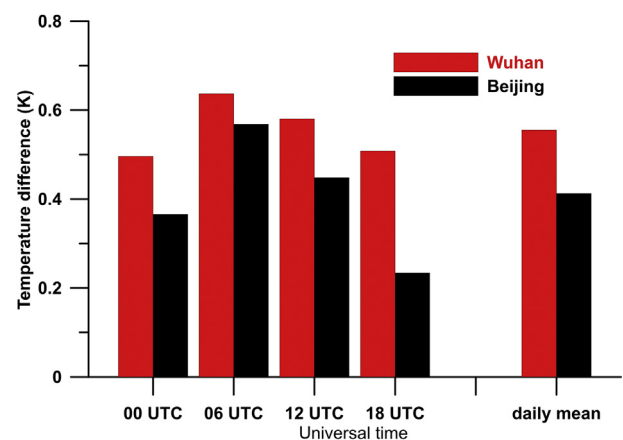


Fig. 7. Mean differences for the first ensemble member (50% reduction experiment aer 1) of the simulated surface air temperatures in Wuhan and Beijing, sorted after the four observations time 00 UTC, 06 UTC, 12 UTC and 18 UTC, and the daily mean, across January to April 2020. The daily mean changes amount to 0.55 K in Wuhan, and 0.41 K in Beijing).

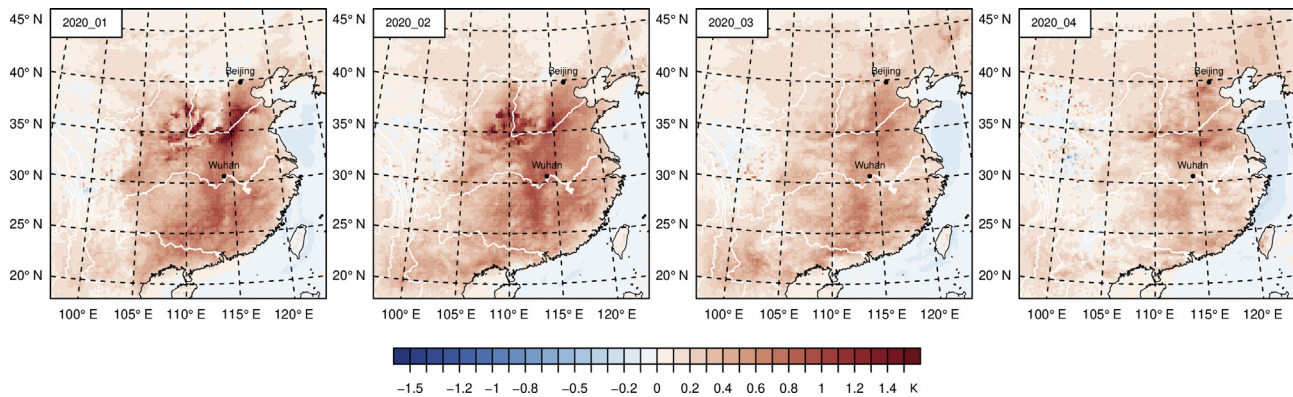


Fig. 8. Change in air temperature in the first pair of experiments,  $\Delta 1$  (aer1–ctl1), for the four considered months, January to April 2020.

As a first test, about the reproduction of the observed state, and of the effect of reducing the aerosol load in the model, we show daily time series of daily mean temperature in Wuhan, from an urban meteorological station, and from the first pair of simulations in Fig. 6. The three curves are all similar, both in phases and intensities. One cannot say if the red (aer 1) or the blue curve (ctl 1) fit better to the black (observed curve). But, the weather stream, as reflected by the day-day-variations in the black curve, are reproduced by the model, in both set-ups. We conclude that the model reproduces the weather stream in January–April 2020 well.

When considering the two simulated curves, besides their general similarity, they exhibit a slight but systematic tendency that the red curve is above the blue curve. Given the large spread of the vertical axis, because of the seasonal change in this period, the changes are not that miniscule as the diagram seems to indicate at first glance.

When the monthly mean differences, sorted after the 4 daily ‘observation times’, 00, 06, 12 and 18 UTC, is calculated, the daily mean differences amount to 0.4–0.5 K with a maximum at 06 UTC, corresponding to 13:00 CST (Fig. 7). That the largest effect coincides with the time of maximum solar radiation is plausible. At other locations, for instance Beijing, the effect of reducing the aerosol load has a marked diurnal cycle (also Fig. 7).

The spatial distribution of the warming as given by the first pair of experiments is shown in Fig. 8: The largest effect is in the Beijing neighborhood, but all of central China is affected. There are strong signals in Shaanxi and Henan as well. However, we assume that this might be an effect of differences in snow cover (not shown), which is quite sensitive to small variations in temperature around 0 °C. The signal weakens in time, with the largest effect in February, or January, and a much-reduced warming in April. This may be an effect of some advective warming earlier in the year, on a weakening of the winter monsoon in particular in the southern parts.

To determine if the results so far are compromised by noteworthy ensemble variability, we had two additional pairs of simulations, as mentioned before. They differ with respect to the first, which we have discussed so far, that the 2nd was

initialized with data from 1 November, and the 3rd with data from 1 July.

Figure 9 shows the daily mean temperature differences in Wuhan for the three simulations. The three developments share a similar overall level and tendency, also the short-term variations are quite similar. The ensemble looks as if generated by a joint development, overlaid with some mostly white noise. In particular the already mentioned gradual weakening of the signal commencing in late March is visible.

A similar result is found for Beijing, albeit with generally smaller differences but without the steady decline of the signal (not shown).

Consistent with the closeness of the time series in Fig. 9, the spatial distributions  $\Delta 2$  and  $\Delta 3$  in Fig. 10 are similar among each other and with that shown in Fig. 8.

After we found essentially the same features also in all three pairs of simulations, we conclude that the warming effect is not a random artifact, but related to the common treatment adopted in the pairs of experiments. The similarity is so obvious that further statistical confirmation, say by a statistical hypothesis testing, is not necessary.<sup>3</sup>

#### 4. Discussion and conclusions

So far, few studies have been done on estimating the climatic effect of the temporal reduction of aerosols following the regional lockdowns (e.g., Weber et al., 2020; Lee et al., 2021). It is long known that the presence of aerosols leads to a lowering of temperatures, thus a warming when fewer aerosols are present (e.g., Li, 2021). A number of studies (e.g., Chen et al., 2018a; 2018b) have been done specifically on effects in East Asia, which describe a significant change in precipitation and circulation apart of temperature. This is different in our study, where we did not find such impacts. This may be related to the fact that we are only considering winter and spring.

<sup>3</sup> Unfortunately, the call for statistical hypothesis testing has become a reflex-action among researchers, who fail to see the inherent limitations of this methodology, cf., Trafimow and Marks (2015).



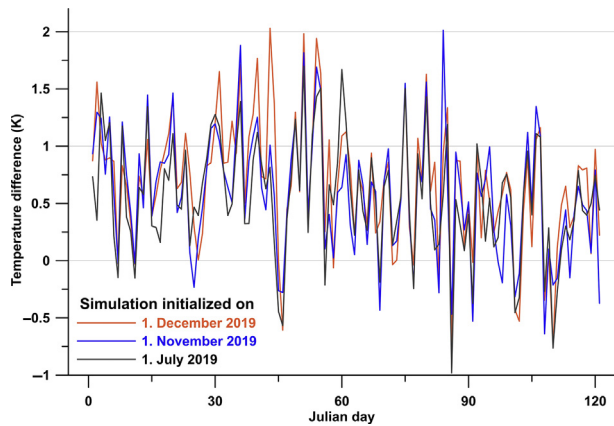


Fig. 9. The ensemble-variability in temperature differences of the 3 pairs of simulations on the impact of reducing the anthropogenic aerosol load by 50% over China. The dates given in the legend refer to the initialization times of the pairs of simulations. Julian days count the days beginning on 1 January.

Our methodology is an ad-hoc approach, in order to assess the consequences of the regional lockdown in a timely manner. To do so, we ran a state-of-the-art regional model subject to assumed reductions of anthropogenic aerosol loads; at the same time we did an analysis of what has been monitored on the ground at a number of stations. It turned out the two approaches lead to consistent estimates.

A problem with the assessment of the observational evidence was that during the last decades there were substantial changes in the regional anthropogenic aerosol loads, which led us to consider only the years 2020, 2019 and 2018. It would be worthwhile to examine our results in light of the years of 2021

and 2022, when the data will become available. A problem with the modelling is that the description of aerosol indirect effects is not mature. Being well aware of both problems, we implemented the two-thronged approach of considering local evidence and modelling.

The main conclusions to be drawn are:

- At selected central China stations temperatures were found to be higher than in the previous two years. This warming goes with a marked diurnal signal. Maximum warming in the early afternoon (06 UTC), weakest at night (18 UTC).
- This may be partly related to a general warming of large swaths of Asia (including Siberia), independently of the regional aerosol forcing. Indeed, also the stations outside the immediate strong lockdown are showing a warming. Thus, the difference (2020 minus 2019/2018) describes a real regional warming, but may overestimate the effect of the reduction of anthropogenic aerosol presence. However, the warming in the industrial region of China is larger than outside, so that effect seems real.
- The ad-hoc numerical experiment indicates that the change caused by the overall reduction of the anthropogenic aerosol optical depth does not lead to phases of larger deviations of local time series in the two simulations. Instead, the simulation with reduced anthropogenic aerosol load shows mostly a mere locally increased temperature. This may indicate that the aerosol effect is almost entirely thermodynamic in all local air columns in the region.
- The observed (local; reanalysis) observations point to an effect of less than 1.0 K, the simulations to a warming of about 0.5 K. This may well be considered as relatively

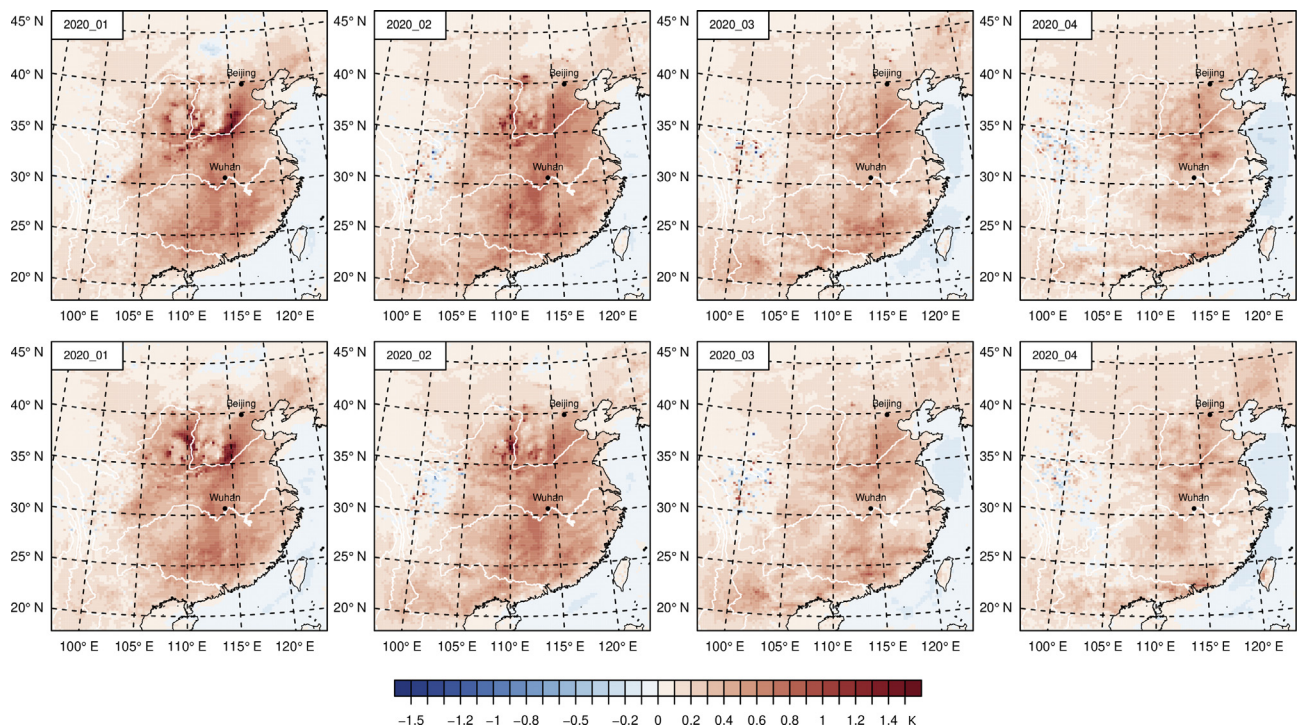


Fig. 10. Change in air temperature for the four considered months, January to April 2020 as in Fig. 8, but for the 2nd (upper) and 3rd (lower) pair of simulations.

small (cf. Weber et al., 2020), but may be helpful to sort out the regional effect of air quality policies on climate change. Note that the uncertainty of these numbers reflects the uncertainty of the large-scale effect as well as the ad-hoc choice of AOD anomaly in the simulations.

## Declaration of competing interest

The authors declare no conflict of interest.

## Acknowledgment

We thank the China Meteorological Administration for sharing the hourly surface air temperature (SAT) series (<http://data.cma.cn>). We enjoyed fruitful discussions with Axel Timmermann. The reanalysis datasets used for this study are from the JRA-55 long-term reanalysis cooperative research project carried out by the Japan Meteorological Agency (JMA) and the Central Research Institute of Electric Power Industry (CRIEPI). The MERRA-2 data used in this study/project have been provided by the Global Modeling and Assimilation Office (GMAO) at NASA Goddard Space Flight Center. The authors acknowledge the collaboration in the CLM-community where the COSMO-CLM is maintained and further development takes place. The German Climate Computing Center (DKRZ) provided the computer hardware for the simulations.

## Appendix A. Supplementary data

Supplementary data to this article can be found online at <https://doi.org/10.1016/j.accre.2021.03.003>.

## References

- Barkhordarian, A., von Storch, H., Zorita, E., et al., 2016. An attempt to deconstruct recent climate change in the Baltic Sea basin. *J. Geophys. Res. Atmos.* <https://doi.org/10.1002/2015JD024648>.
- Bucchignani, E., Montesarchio, M., Cattaneo, L., et al., 2014. Regional climate modeling over China with COSMO-CLM: performance assessment and climate projections. *J. Geophys. Res. Atmos.* 119 (21), 12–151. <https://doi.org/10.1002/2014JD022219>, 170.
- Bucchignani, E., Zollo, A.L., Cattaneo, L., et al., 2017. Extreme weather events over China: assessment of COSMO-CLM simulations and future scenarios. *Int. J. Climatol.* 37, 1578–1594. <https://doi.org/10.1002/joc.4798>.
- Cao, S., He, L., Shen, X., et al., 2020. Chinese. Analysis of the February 2020: atmospheric circulation and weather. *Meteorol. Mon.* 46, 725–732 doi: 10.751/19/j.issn.1000-526.2020.05.13 (Chinese).
- Chen, G., Wang, W.C., Chen, J.P., 2018a. Circulation responses to regional aerosol climate forcing in summer over East Asia. *Clim. Dynam.* 51, 3973–3978. <https://doi.org/10.1007/s00382-018-4267-3>.
- Chen, G., Yang, J., Bao, Q., et al., 2018b. Intraseasonal responses of the East Asia summer rainfall to anthropogenic aerosol climate forcing. *Clim. Dynam.* 51, 3985–3998. <https://doi.org/10.1007/s00382-017-3691-0>.
- Chin, M., Ginoux, P., Kinne, S., et al., 2002. Tropospheric aerosol optical thickness from the GOCART model and comparisons with satellite and sun photometer measurements. *J. Atmos. Sci.* 59, 461–483. [https://doi.org/10.1175/1520-0469\(2002\)059<0461:TAOTFT>2.0.CO;2](https://doi.org/10.1175/1520-0469(2002)059<0461:TAOTFT>2.0.CO;2).
- Davies, H.C., 1976. A lateral boundary formulation for multi-level prediction models. *Q. J. R. Meteorol. Soc.* 102, 405–418. <https://doi.org/10.1002/qj.49710243210>.
- Gelaro, R., McCarty, W., Suárez, M.J., et al., 2017. The modern-Era Retrospective analysis for research and applications, version 2 (MERRA-2). *J. Clim.* 30, 5419–5454. <https://doi.org/10.1175/jcli-d-16-0758.1>.
- Geyer, B., Ludwig, T., von Storch, H., 2020. Limits of reproducibility and hydrodynamic noise in atmospheric regional modelling. *Commun. Earth Environ.* 2 (17) <https://doi.org/10.1038/s43247-020-00085-4>.
- Guan, L., Zhang, T., Liu, Z., 2020. Chinese. Analysis of the April 2020: atmospheric circulation and weather. *Meteorol. Mon.* 46, 994–1000. <https://doi.org/10.7519/j.issn.1000-0526.2020.07.011> (Chinese).
- He, G., Pan, Y., Tanaka, T., 2020. The short-term impacts of COVID-19 lockdown on urban air pollution in China. *Nat. Sustain.* <https://doi.org/10.1038/s41893-020-0581-y>.
- Holben, B., Eck, T., Slutsker, I., et al., 1998. AERONET: a federated instrument network and data archive for aerosol characterization. *Remote Sens. Environ.* 66, 1–16. [https://doi.org/10.1016/S0034-4257\(98\)00031-5](https://doi.org/10.1016/S0034-4257(98)00031-5).
- Hong, C., Zhang, Q., Zhang, Y., et al., 2020. Weakening aerosol direct radiative effects mitigate climate penalty on Chinese air quality. *Nat. Clim. Change* 10, 845–850.
- Jiang, Q., Gui, H., Xu, R., 2020. Chinese. Analysis of January 2020: atmospheric circulation and weather. *Meteorol. Mon.* 46, 575–580. <https://doi.org/10.7519/j.issn.1000-0526.2020.04.012>.
- Jung, J., Souri, A.H., Wong, D.C., et al., 2019. The impact of the direct effect of aerosols on meteorology and air quality using aerosol optical depth assimilation during the KORUS-AQ campaign. *J. Geophys. Res. Atmos.* 124, 8303–8319. <https://doi.org/10.1029/2019JD030641>.
- Kinne, S., O'Donnell, D., Stier, P., et al., 2013. MAC-v1: a new global aerosol climatology for climate studies. *J. Adv. Model. Earth Syst.* 5, 704–740. <https://doi.org/10.1002/jame.20035>.
- Kobayashi, S., Ota, Y., Harada, Y., et al., 2015. The JRA-55 reanalysis: general specifications and basic characteristics. *J. Meteorol. Soc. Japan. Ser. II* 93, 5–48. <https://doi.org/10.2151/jmsj.2015-001>.
- Lee, S.S., Chu, J.E., Timmermann, A., et al., 2021. East Asian climate response to COVID-19 lockdown measures in China. *Sci Rep* 11, 16852. <https://doi.org/10.1038/s41598-021-96007-1>.
- Li, D., 2017. Added value of high-resolution regional climate model: selected cases over the Bohai Sea and the Yellow Sea areas. *Int. J. Climatol.* 37 (1) <https://doi.org/10.1002/joc.4695>.
- Li, D., Geyer, B., Bisling, P., 2016a. A model-based climatology analysis of wind power resources at 100-m height over the Bohai Sea and the Yellow Sea. *Appl. Energy* 179, 575–589. <https://doi.org/10.1016/j.apenergy.2016.07.010>.
- Li, D., von Storch, H., Geyer, B., 2016b. High-resolution wind hindcast over the Bohai sea and the Yellow Sea in East Asia: evaluation and wind climatology analysis. *J. Geophys. Res. Atmos.* 121, 111–129. <https://doi.org/10.1002/2015JD024177>, 2015JD024177.
- Li, D., Yin, B., Feng, J., et al., 2018. Present climate evaluation and added value analysis of dynamically downscaled simulations of CORDEX: East Asia. *J. Appl. Meteorol. Climatol.* 57, 2317–2341. <https://doi.org/10.1175/JAMC-D-18-0008.1>.
- Li, D., Staneva, J., Grayek, S., et al., 2020. Skill assessment of an atmosphere – wave regional coupled model over the East China Sea with a focus on typhoons. *Atmosphere* 11 (3), 252. <https://doi.org/10.3390/atmos11030252>, 2020.
- Li, K., 2021. Climate change and aerosol sciences. *J. Earth Sci. Geotech. Eng.* 11 (1), 1–13. <https://doi.org/10.47260/jesge/1131>, 2021.
- McCartney, E.J., 1976. *Optics of the Atmosphere: Scattering by Molecules and Particles*. Wiley series in pure and applied optics. Wiley, New York.
- Ritter, B., Geleyn, J.-F., 1992. A comprehensive radiation scheme for numerical weather prediction models with potential applications in climate simulations. *Mon. Weather Rev.* 120, 303–325. [https://doi.org/10.1175/1520-0493\(1992\)120<0303:ACRSFN>2.0.CO;2](https://doi.org/10.1175/1520-0493(1992)120<0303:ACRSFN>2.0.CO;2).
- Rockel, B., Will, A., Hense, A., 2008. The regional climate model COSMO-CLM (CCLM). *Meteorol. Z.* 17, 347–348. <https://doi.org/10.1127/0941-2948/2008/0309>.
- Rugani, B., Caro, D., 2020. Impact of COVID-19 outbreak measures of lockdown on the Italian carbon footprint. *Sci. Total Environ.* 737, 139806. <https://doi.org/10.1016/j.scitotenv.2020.139806>.
- Schultze, M., Rockel, B., 2018. Direct and semi-direct effects of aerosol climatologies on long-term climate simulations over Europe.



- Clim. Dynam. 50, 3331–3354. <https://doi.org/10.1007/s00382-017-3808-5>.
- Steppeler, J., Doms, G., Schättler, U., et al., 2003. Meso-gamma scale forecasts using the nonhydrostatic model LM. Meteorol. Atmos. Phys. 82, 75–96. <https://doi.org/10.1007/s00703-001-0592-9>.
- Trafimow, D., Marks, M., 2015. Editorial. Basic Appl. Soc. Psychol. 37, 1–2. <https://doi.org/10.1080/01973533.2015.1012991>.
- Wang, D., Menz, C., Simon, T., et al., 2013. Regional dynamical downscaling with CCLM over East Asia. Meteorol. Atmos. Phys. 121, 39–53. <https://doi.org/10.1007/s00703-013-0250-z>.
- Weber, J., Shin, Y.M., Staunton Sykes, J., et al., 2020. Minimal climate impacts from short-lived climate forcers following emission reductions related to the COVID-19 pandemic. Geophys. Res. Lett. 47, e2020GL090326. <https://doi.org/10.1029/2020GL090326>.
- Weisse, R., Heyen, H., Storch, H.v., 2000. Sensitivity of a regional atmospheric model to a sea state-dependent roughness and the need for ensemble calculations. Mon. Weather Rev. 128, 3631–3642.
- Yu, K., Hui, P., Zhou, W., et al., 2020. Evaluation of multi-RCM high-resolution hindcast over the CORDEX east Asia phase II region: mean, annual cycle and interannual variations. Int. J. Climatol. 40, 2134–2152. <https://doi.org/10.1002/joc.6323>.
- Yue, X., Lei, Y., Zhou, H., et al., 2020. Changes of anthropogenic carbon emissions and air pollutants during the COVID-19 epidemic in China. Transact. Atmospher. Sci., 43. <https://doi.org/10.13878/j.cnki.dqkxxb.20200408010>.
- Zhou, W., Tang, J., Wang, X., et al., 2016. Evaluation of regional climate simulations over the CORDEX-EA-II domain using the COSMO-CLM model. Asia-Pac. J. Atmos. Sci. 52, 107–127. <https://doi.org/10.1007/s13143-016-0013-0>.
- Zhou, X., Zhang, T., 2020. Analysis of the March 2020: atmospheric circulation and weather. Meteorol. Mon. 46, 863–872. <https://doi.org/10.7519/j.issn.1000-0526.2020.06.013> (Chinese).